

Article

A Global, 0.05-Degree Product of Solar-Induced Chlorophyll Fluorescence Derived from OCO-2, MODIS, and Reanalysis Data

Xing Li and Jingfeng Xiao *

Earth Systems Research Center, Institute for the Study of Earth, Oceans, and Space, University of New Hampshire, Durham, NH 03824, USA; zxwlxty@163.com

* Correspondence: j.xiao@unh.edu; +1-603-862-1873

Received: 20 January 2019; Accepted: 27 February 2019; Published: 4 March 2019

Abstract: Solar-induced chlorophyll fluorescence (SIF) brings major advancements in measuring terrestrial photosynthesis. Several recent studies have evaluated the potential of SIF retrievals from the Orbiting Carbon Observatory-2 (OCO-2) in estimating gross primary productivity (GPP) based on GPP data from eddy covariance (EC) flux towers. However, the spatially and temporally sparse nature of OCO-2 data makes it challenging to use these data for many applications from the ecosystem to the global scale. Here, we developed a new global ‘OCO-2’ SIF data set (GOSIF) with high spatial and temporal resolutions (i.e., 0.05°, 8-day) over the period 2000–2017 based on a data-driven approach. The predictive SIF model was developed based on discrete OCO-2 SIF soundings, remote sensing data from the Moderate Resolution Imaging Spectroradiometer (MODIS), and meteorological reanalysis data. Our model performed well in estimating SIF ($R^2 = 0.79$, root mean squared error (RMSE) = 0.07 $\text{W m}^{-2} \mu\text{m}^{-1} \text{sr}^{-1}$). The model was then used to estimate SIF for each 0.05° × 0.05° grid cell and each 8-day interval for the study period. The resulting GOSIF product has reasonable seasonal cycles, and captures the similar seasonality as both the coarse-resolution OCO-2 SIF (1°), directly aggregated from the discrete OCO-2 soundings, and tower-based GPP. Our SIF estimates are highly correlated with GPP from 91 EC flux sites ($R^2 = 0.73$, $p < 0.001$). They capture the expected spatial and temporal patterns and also have remarkable ability to highlight the crop areas with the highest daily productivity across the globe. Our product also allows us to examine the long-term trends in SIF globally. Compared with the coarse-resolution SIF that was directly aggregated from OCO-2 soundings, GOSIF has finer spatial resolution, globally continuous coverage, and a much longer record. Our GOSIF product is valuable for assessing terrestrial photosynthesis and ecosystem function, and benchmarking terrestrial biosphere and Earth system models.

Keywords: solar-induced chlorophyll fluorescence; Orbiting Carbon Observatory-2; Moderate Resolution Imaging Spectroradiometer; gross primary productivity; photosynthesis; machine learning; data-driven approach; carbon cycle; trend; benchmarking; FLUXNET

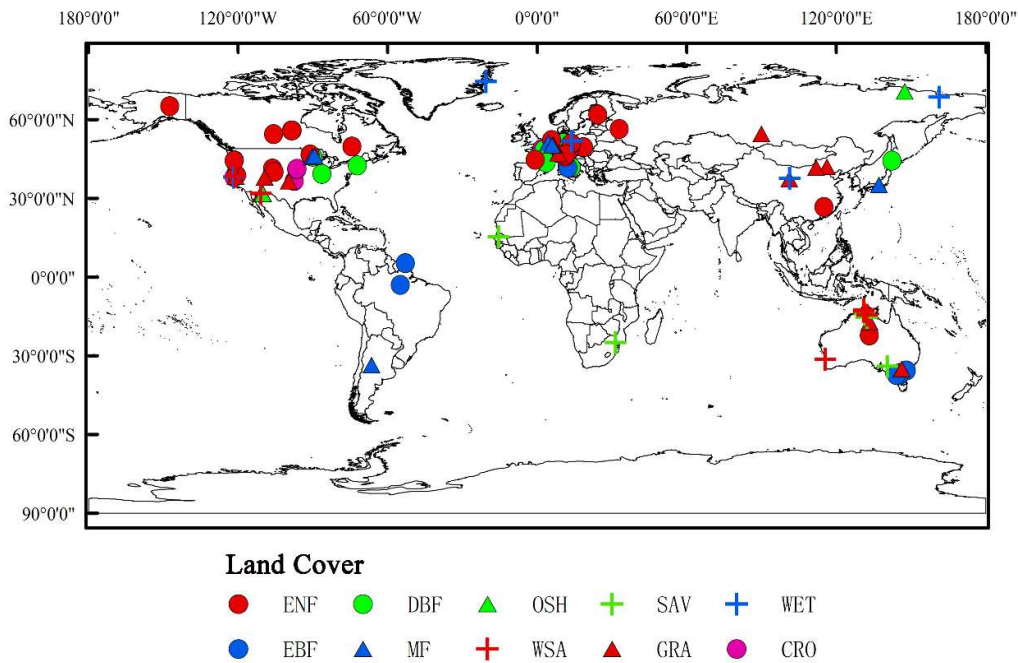


Figure 1. The spatial distribution and land cover types of the 91 eddy covariance (EC) flux sites from the FLUXNET 2015 Tier 1 dataset used in this study.

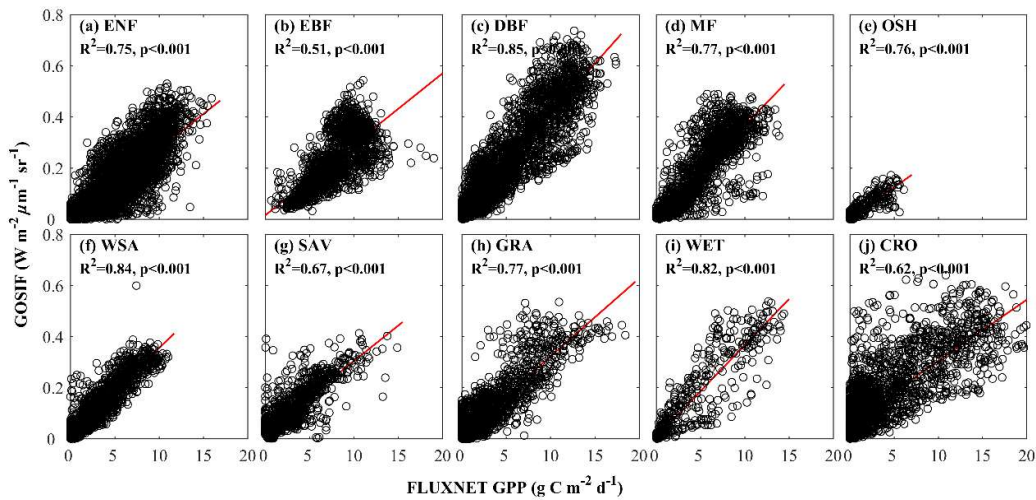


Figure 2. Relationship between solar-induced chlorophyll fluorescence (SIF) from our global Orbiting Carbon Observatory-2 SIF (GOSIF) product and gross primary productivity (GPP) from the FLUXNET 2015 Tier 1 dataset across biomes. The R^2 for each biome is as follows: Evergreen needleleaf forests (0.75), evergreen broadleaf forests (0.51), deciduous broadleaf forests (0.85), mixed forests (0.77), open shrublands (0.76), woody savannas (0.84), savannas (0.67), grasslands (0.77), wetlands (0.82), and croplands (0.62). The p value for each biome is less than 0.001.

Table S1. The statistical measures for model development and validation. Model 1 is based on surface reflectance of Moderate Resolution Imaging Spectroradiometer (MODIS) bands 1–7, Model 2 is based on MODIS bands 1–7 and meteorological data (photosynthetically active radiation or PAR, vapor pressure deficit or VPD, and temperature), and Model 3 is based on enhanced vegetation index (EVI) and meteorological data (PAR, VPD, and temperature). The inclusion of meteorological data could improve the estimation of SIF, and the use of EVI, PAR, VPD, and temperature (Model 2) had a slightly higher performance than the use of MODIS bands 1–7 (Model 1) and an identical performance with the use of MODIS bands 1–7 and three meteorological variables (Model 3).

	Fitting		Cross-validation		
	Average Error	Relative Error	R	RMSE	R ²
Model 1	0.05	0.46	0.86	0.07	0.70
Model 2	0.04	0.40	0.90	0.06	0.77
Model 3	0.04	0.43	0.88	0.06	0.77

Table 2. FLUXNET Tier-1 sites used for evaluating GOSIF in this study. Site descriptions includes site code (Column 1), site name (Column 2), Biome type (Column 3), years of data available (Column 4), latitude (Column 5), longitude (Column 6), R² (SIF versus FLUXNET GPP), and references (Column 8) for each flux site. We used the average of night-time (GPP_NT_VUT_REF) and day-time (GPP_DT_VUT_REF) estimates to evaluate the GOSIF. GPP_NT_VUT_REF: GPP from the nighttime (NT) partitioning method, using the Variable Ustar Threshold filtering method, reference selected from GPP versions using model efficiency (MEF). DT indicates the daytime partitioning method.

Site-code	Site-Name	Biome	Year	Lat	Lon	R ²	References
AR-Slu	San Luis	MF	2009–2011	-33.4648	-66.4598	0.65	
AU-Ade	Adelaide River	WSA	2007–2009	-13.0769	131.1178	0.74	
AU-ASM	Alice Springs	ENF	2010–2013	-22.2830	133.2490	0.79	
AU-Cpr	Calperum	SAV	2010–2014	-34.0021	140.5891	0.78	[1]
AU-Das	Daly River Cleared	SAV	2008–2014	-14.1593	131.3880	0.69	[1]
AU-Dry	Dry River	SAV	2008–2014	-15.2588	132.3706	0.55	[2]
AU-Emr	Emerald	GRA	2011–2013	-23.8587	148.4746	0.58	[3]
AU-Gin	Gingin	WSA	2011–2014	-31.3764	115.7138	0.62	[1]
AU-How	Howard Springs	WSA	2001–2014	-12.4952	131.1501	0.75	[4]
AU-RDF	Red Dirt Melon Farm, Northern Territory	WSA	2011–2013	-14.5636	132.4776	0.38	
AU-Rig	Riggs Creek	CRO	2011–2014	-36.6499	145.5759	0.80	
AU-Stp	Sturt Plains	GRA	2008–2014	-17.1508	133.3503	0.80	[4]
AU-TUM	Tumbarumba	EBF	2001–2014	-35.6566	148.1516	0.61	[5]
AU-Wac	Wallaby Creek	EBF	2005–2008	-37.4259	145.1878	0.45	
AU-Wom	Wombat	EBF	2010–2012	-37.4222	144.0944	0.82	
AU-ync	Jaxa	GRA	2012–2014	-34.9893	146.2907	0.87	
BE-Bra	Brasschaat	MF	2000–2014	51.3092	4.5206	0.83	[6]
BE-Vie	Vielsalm	MF	2000–2014	50.3051	5.9981	0.92	[7]
BR-Sa3	Santarem-Km83-Logged Forest	EBF	2000–2004	-3.0180	-54.9714	0.16	[8]
CA-Man	Manitoba - Northern Old Black Spruce	ENF	2000–2014	55.8800	-98.4810	0.85	
CA-NS2	UCI-1930 burn site	ENF	2001–2005	55.9058	-98.5247	0.87	
CA-NS3	UCI-1964 burn site	ENF	2001–2005	55.9117	-98.3822	0.86	[9]
CA-NS4	UCI-1964 burn site wet	ENF	2002–2005	55.9144	-98.3806	0.94	[10]
CA-NS5	UCI-1981 burn site	ENF	2001–2005	55.8631	-98.4850	0.93	
CA-Qfo	Quebec - Eastern Boreal, Mature Black Spruce	ENF	2003–2010	49.6925	-74.3420	0.91	[11]
CA-SF1	Saskatchewan - Western Boreal, forest burned in 1977	ENF	2003–2006	54.4850	-105.8176	0.67	[12]

CH-Cha	Chamau	GRA	2005–2014	47.2102	8.4104	0.74	[13]
CH-Dav	Davos	ENF	2000–2014	46.8153	9.8559	0.55	
CN-Du2	Duolun_grassland (D01)	GRA	2006–2008	42.0467	116.2836	0.77	[14]
CN-Ha2	Haibei Shrubland	WET	2003–2005	37.6086	101.3269	0.95	[15]
CN-Ham	Haibei Alpine Tibet site	GRA	2002–2004	37.3700	101.1800	0.91	[16]
CN-Qia	Qianyanzhou	ENF	2003–2005	26.7414	115.0581	0.81	[17]
CN-Sw2	Siziwang Grazed (SZWG)	GRA	2010–2012	41.7902	111.8971	0.00	[18]
CZ-BK1	Bily Kriz forest	ENF	2004–2008	49.5021	18.5369	0.65	[19]
DE-Geb	Gebesee	CRO	2001–2014	51.1001	10.9143	0.65	
DE-Hai	Hainich	DBF	2000–2012	51.0792	10.4530	0.88	[20]
DE-Kli	Klingenberg	CRO	2004–2014	50.8929	13.5225	0.64	[21]
DE-lkb	Lackenberg	ENF	2009–2013	49.0996	13.3047	0.91	[22]
DE-Obe	Oberbärenburg	ENF	2008–2014	50.7836	13.7196	0.82	
DE-RUR	Rollesbroich	GRA	2011–2014	50.6219	6.3041	0.80	[23]
DE-Spw	Spreewald	WET	2010–2014	51.8923	14.0337	0.95	
DK-Tha	Tharandt	ENF	2000–2014	50.9636	13.5669	0.86	[108]
DK-ZaF	Zackenberg Fen	WET	2008–2011	74.4814	-20.5545	0.65	
FI-Hyy	Hyytiala	ENF	2000–2014	61.8475	24.2950	0.90	[24, 25]
FR-Fon	Fontainebleau-Barbeau	DBF	2005–2014	48.4764	2.7801	0.67	[26]
FR-Gri	Grignon	CRO	2004–2013	48.8442	1.9519	0.48	[27]
FR-Lbr	Le Bray	ENF	2000–2008	44.7171	-0.7693	0.72	
FR-Pue	Puechabon	DBF	2000–2014	43.7414	3.5958	0.39	[28]
GF-Guy	Guyaflux (French Guiana)	EBF	2004–2014	5.2788	-52.9249	0.00	[29]
IT-CA2	Castel d'Asso2	CRO	2011–2014	42.3772	12.0260	0.49	[30]
IT-Col	Collelongo	DBF	2000–2014	41.8494	13.5881	0.90	
IT-Cpz	Castelporziano	EBF	2000–2009	41.7052	12.3761	0.61	
IT-Lav	Lavarone	ENF	2003–2014	45.9562	11.2813	0.68	[31]
IT-Ren	Renon	ENF	2002–2013	46.5869	11.4337	0.90	[32]
JP-MBF	Moshiri Birch Forest Site	DBF	2003–2005	44.3869	142.3186	0.93	
JP-SMF	Seto Mixed Forest Site	MF	2002–2006	35.2500	137.0667	0.85	
NL-Loo	Loobos	ENF	2000–2013	52.1666	5.7436	0.89	[33]
RU-Che	Cherski	WET	2002–2005	68.6130	161.3414	0.75	[34]
RU-Cok	Chokurdakh	OSH	2003–2014	70.8291	147.4943	0.68	[35]

RU-Fyo	Fyodorovskoye	ENF	2000–2014	56.4615	32.9221	0.85	[36]
RU-Ha1	Hakasia steppe	GRA	2002–2004	54.7252	90.0022	0.92	
SD-Dem	Demockeya	SAV	2005–2009	13.2829	30.4783	0.54	[37]
SN-Dhr	Dahra	SAV	2010–2013	15.4028	-15.4322	0.87	
US-AR2	ARM USDA UNL OSU Woodward Switchgrass 2	GRA	2009–2012	36.6358	-99.5975	0.51	
US-Arm	ARM Southern Great Plains site- Lamont	CRO	2003–2012	36.6058	-97.4888	0.62	[38]
US-Blo	Blodgett Forest	ENF	2000–2007	38.8953	-120.6328	0.72	[39]
US-Cop	Corral Pocket	GRA	2001–2007	38.0900	-109.3900	0.19	
US-GLE	GLEES	ENF	2005–2014	41.3644	-106.2394	0.83	
US-Ha1	Harvard Forest EMS Tower (HFR1)	DBF	2000–2012	42.5378	-72.1715	0.94	[40]
US-Me2	Metolius mature ponderosa pine	ENF	2002–2014	44.4523	-121.5574	0.73	[41]
US-ME6	Metolius Young Pine Burn	ENF	2010–2014	44.3232	-121.6043	0.52	[41]
US-MMS	Morgan Monroe State Forest	DBF	2000–2014	39.3232	-86.4131	0.94	[42]
US-Ne1	Mead - irrigated continuous maize site	CRO	2001–2013	41.1651	-96.4766	0.83	[43]
US-Ne2	Mead - irrigated maize-soybean rotation site	CRO	2001–2013	41.1649	-96.4701	0.77	[43]
US-Ne3	Mead - rainfed maize-soybean rotation site	CRO	2001–2013	41.1797	-96.4396	0.77	[44]
US-NR1	Niwot Ridge Forest (LTER NWT1)	ENF	2000–2014	40.0329	-105.5464	0.84	[45]
US-Pfa	Park Falls/WLEF	MF	2000–2014	45.9459	-90.2723	0.91	[46]
US-Prr	Poker Flat Research Range Black Spruce Forest	ENF	2010–2013	65.1237	-147.4876	0.84	
US-SRG	Santa Rita Grassland	GRA	2008–2014	31.7894	-110.8277	0.79	[47]
US-SRM	Santa Rita Mesquite	WSA	2004–2014	31.8214	-110.8661	0.83	[48]
US-Syv	Sylvania Wilderness Area	MF	2001–2014	46.2420	-89.3477	0.95	[49]
US-Ton	Tonzi Ranch	WSA	2001–2014	38.4316	-120.9660	0.79	[50]
US-Tw1	Twitchell Wetland West Pond	WET	2012–2014	38.1074	-121.6469	0.77	
US-Twt	Twitchell Island	CRO	2009–2014	38.1055	-121.6521	0.76	[51]
US-Var	Vaira Ranch- Ione	GRA	2000–2014	38.4067	-120.9507	0.59	[52]
US-Wcr	Willow Creek	DBF	2000–2014	45.8059	-90.0799	0.95	[53]
US-whs	Walnut Gulch Lucky Hills Shrub	OSH	2007–2014	31.7438	-110.0522	0.77	[54]
US-Wi3	Mature hardwood (MHW)	DBF	2002–2004	46.6347	-91.0987	0.96	
US-Wi4	Mature red pine (MRP)	ENF	2002–2005	46.7393	-91.1663	0.81	
US-Wkg	Walnut Gulch Kendall Grasslands	GRA	2004–2014	31.7365	-109.9419	0.76	[55]
ZA-Kru	Skukuza	SAV	2000–2010	-25.0197	31.4969	0.63	[56]

References

- Beringer, J.; L.B. Hutley; I. McHugh; S.K. Arndt; D. Campbell; H.A. Cleugh; J. Cleverly; V. Resco de Dios; D. Eamus; B. Evans. An introduction to the Australian and New Zealand flux tower network—OzFlux. *Biogeosciences*. **2016**.
- Beringer, J.; L.B. Hutley; J.M. Hacker; B. Neininger. Patterns and processes of carbon, water and energy cycles across northern Australian landscapes: From point to region. *Agric. For. Meteorol.* **2011**, *151*, 1409–1416.
- Etheridge, D.; R. Gregory; C. Allison; T. Kuske; H. Berko; I. Schroder; Z. Loh; A.J. Feitz; M. Hibberd; S. Zegelin, *Metadata report: Arcturus atmospheric greenhouse gas monitoring*. 2014: Geoscience Australia.
- Beringer, J.; J. Hacker; L.B. Hutley; R. Leuning; S.K. Arndt; R. Amiri; L. Bannehr; L.A. Cernusak; S. Grover; C. Hensley. SPECIAL—Savanna patterns of energy and carbon integrated across the landscape. *Bull. Am. Meteorol. Soc.* **2011**, *92*, 1467–1485.
- Leuning, R.; H.A. Cleugh; S.J. Zegelin; D. Hughes. Carbon and water fluxes over a temperate Eucalyptus forest and a tropical wet/dry savanna in Australia: measurements and comparison with MODIS remote sensing estimates. *Agric. For. Meteorol.* **2005**, *129*, 151–173.
- Janssens, I.A.; A.S. Kowalski; R. Ceulemans. Forest floor CO₂ fluxes estimated by eddy covariance and chamber-based model. *Agric. For. Meteorol.* **2001**, *106*, 61–69.
- Aubinet, M.; B. Chermant; M. Vandenhaute; B. Longdoz; M. Yernaux; E. Laitat. Long term carbon dioxide exchange above a mixed forest in the Belgian Ardennes. *Agric. For. Meteorol.* **2001**, *108*, 293–315.
- Steininger, M.K. Net carbon fluxes from forest clearance and regrowth in the Amazon. *Ecol. Appl.* **2004**, *14*, 313–322.
- Goulden, M.L.; G.C. Winston; A.M. McMillan; M.E. Litvak; E.L. Read; A.V. Rocha; J. Rob Elliot. An eddy covariance mesonet to measure the effect of forest age on land–atmosphere exchange. *Glob. Chang. Biol.* **2006**, *12*, 2146–2162.
- Bond-Lamberty, B.; C. Wang; S.T. Gower. Net primary production and net ecosystem production of a boreal black spruce wildfire chronosequence. *Glob. Chang. Biol.* **2004**, *10*, 473–487.
- Bergeron, O.; H.A. Margolis; T.A. Black; C. Courtsolle; A.L. Dunn; A.G. Barr; S.C. Wofsy. Comparison of carbon dioxide fluxes over three boreal black spruce forests in Canada. *Glob. Chang. Biol.* **2007**, *13*, 89–107.
- Amiro, B.; A. Orchansky; A. Barr; T. Black; S. Chambers; F. Chapin III; M. Goulden; M. Litvak; H. Liu; J. McCaughey. The effect of post-fire stand age on the boreal forest energy balance. *Agric. For. Meteorol.* **2006**, *140*, 41–50.
- Eugster, W.; M.J. Zeeman. *Micrometeorological techniques to measure ecosystem-scale greenhouse gas fluxes for model validation and improvement*. in *International Congress Series*. 2006. Elsevier.
- Sun, G.; K. Alstad; J. Chen; S. Chen; C.R. Ford; G. Lin; C. Liu; N. Lu; S.G. McNulty; H. Miao. A general predictive model for estimating monthly ecosystem evapotranspiration. *Ecohydrology*. **2011**, *4*, 245–255.
- Li, H.; F. Zhang; Y. Li; J. Wang; L. Zhang; L. Zhao; G. Cao; X. Zhao; M. Du. Seasonal and inter-annual variations in CO₂ fluxes over 10 years in an alpine shrubland on the Qinghai-Tibetan Plateau, China. *Agric. For. Meteorol.* **2016**, *228*, 95–103.
- Kato, T.; Y. Tang; S. Gu; M. Hirota; M. Du; Y. Li; X. Zhao. Temperature and biomass influences on interannual changes in CO₂ exchange in an alpine meadow on the Qinghai-Tibetan Plateau. *Glob. Chang. Biol.* **2006**, *12*, 1285–1298.
- Zhang, L.; Y. Luo; G. Yu; L. Zhang. Estimated carbon residence times in three forest ecosystems of eastern China: Applications of probabilistic inversion. *J. Geophys. Res. Biogeosci.* **2010**, *115*.
- Shao, C.; J. Chen; L. Li. Grazing alters the biophysical regulation of carbon fluxes in a desert steppe. *Environ. Res. Lett.* **2013**, *8*, 025012.
- Marek, M.V.; D. Janouš; K. Taufarová; K. Havránková; M. Pavelka; V. Kaplan; I. Marková. Carbon exchange between ecosystems and atmosphere in the Czech Republic is affected by climate factors. *Environ. Pollut.* **2011**, *159*, 1035–1039.
- Anthoni, P.; A. Knohl; C. Rebmann; A. Freibauer; M. Mund; W. Ziegler; O. Kolle; E.D. Schulze. Forest and agricultural land-use-dependent CO₂ exchange in Thuringia, Germany. *Glob. Chang. Biol.* **2004**, *10*, 2005–2019.
- Prescher, A.-K.; T. Grünwald; C. Bernhofer. Land use regulates carbon budgets in eastern Germany: From NEE to NBP. *Agric. For. Meteorol.* **2010**, *150*, 1016–1025.
- Lindauer, M.; H. Schmid; R. Grote; M. Mauder; R. Steinbrecher; B. Wolpert. Net ecosystem exchange over a non-cleared wind-throw-disturbed upland spruce forest—Measurements and simulations. *Agric. For. Meteorol.* **2014**, *197*, 219–234.
- Post, H.; H.-J. Hendriks Franssen; A. Graf; M. Schmidt; H. Vereecken. Uncertainty analysis of eddy covariance CO₂ flux measurements for different EC tower distances using an extended two-tower

- approach. *Biogeosciences*. **2015**, *12*, 1205–1221.
- 24. Kolari, P.; L. Kulmala; J. Pumpanen; S. Launiainen; H. Ilvesniemi; P. Han; E. Nikinmaa. CO₂ exchange and component CO₂ fluxes of a boreal Scots pine forest. *Boreal Environ. Res.* **2009**, *14*.
 - 25. Mammarella, I.; S. Launiainen; T. Gronholm; P. Keronen; J. Pumpanen; Ü. Rannik; T. Vesala. Relative humidity effect on the high-frequency attenuation of water vapor flux measured by a closed-path eddy covariance system. *JAtOT*. **2009**, *26*, 1856–1866.
 - 26. Delpierre, N.; D. Berveiller; E. Granda; E. Dufrêne. Wood phenology, not carbon input, controls the interannual variability of wood growth in a temperate oak forest. *New Phytol.* **2016**, *210*, 459–470.
 - 27. Loubet, B.; P. Laville; S. Lehuger; E. Larmanou; C. Fléchard; N. Mascher; S. Genermont; R. Roche; R.M. Ferrara; P. Stella. Carbon, nitrogen and Greenhouse gases budgets over a four years crop rotation in northern France. *Plant Soil*. **2011**, *343*, 109.
 - 28. Lhomme, J.-P.; A. Rocheteau; J. Ourcival; S. Rambal. Non-steady-state modelling of water transfer in a Mediterranean evergreen canopy. *Agric. For. Meteorol.* **2001**, *108*, 67–83.
 - 29. Epron, D.; A. Bosc; D. Bonal; V. Freycon. Spatial variation of soil respiration across a topographic gradient in a tropical rain forest in French Guiana. *J. Trop. Ecol.* **2006**, *22*, 565–574.
 - 30. Sabbatini, S.; N. Arriga; T. Bertolini; S. Castaldi; T. Chiti; C. Consalvo; S.N. Djomo; B. Gioli; G. Matteucci; D. Papale. Greenhouse gas balance of cropland conversion to bioenergy poplar short-rotation coppice. *Biogeosciences*. **2016**, *13*, 95–113.
 - 31. Fiora, A.; A. Cescatti. Diurnal and seasonal variability in radial distribution of sap flux density: implications for estimating stand transpiration. *Tree Physiol.* **2006**, *26*, 1217–1225.
 - 32. Marcolla, B.; A. Cescatti; L. Montagnani; G. Manca; G. Kerschbaumer; S. Minerbi. Importance of advection in the atmospheric CO₂ exchanges of an alpine forest. *Agric. For. Meteorol.* **2005**, *130*, 193–206.
 - 33. Dolman, A.; E. Moors; J. Elbers. The carbon uptake of a mid latitude pine forest growing on sandy soil. *Agric. For. Meteorol.* **2002**, *111*, 157–170.
 - 34. Corradi, C.; O. Kolle; K. Walter; S. Zimov; E.D. Schulze. Carbon dioxide and methane exchange of a north-east Siberian tussock tundra. *Glob. Chang. Biol.* **2005**, *11*, 1910–1925.
 - 35. Van Huissteden, J.; T. Maximov; A. Dolman. High methane flux from an arctic floodplain (Indigirka lowlands, eastern Siberia). *J. Geophys. Res. Biogeosci.* **2005**, *110*.
 - 36. Milyukova, I.M.; O. Kolle; A.V. Varlagin; N.N. Vygodskaya; E.D. SCHULZE; J. Lloyd. Carbon balance of a southern taiga spruce stand in European Russia. *Tellus B*. **2002**, *54*, 429–442.
 - 37. Ardö, J.; M. Mölder; B.A. El-Tahir; H.A.M. Elkhidir. Seasonal variation of carbon fluxes in a sparse savanna in semi arid Sudan. *Carbon Balance Manage.* **2008**, *3*, 7.
 - 38. Fischer, M.L.; D.P. Billesbach; J.A. Berry; W.J. Riley; M.S. Torn. Spatiotemporal variations in growing season exchanges of CO₂, H₂O, and sensible heat in agricultural fields of the Southern Great Plains. *Earth Interactions*. **2007**, *11*, 1–21.
 - 39. Misson, L.; J. Tang; M. Xu; M. McKay; A. Goldstein. Influences of recovery from clear-cut, climate variability, and thinning on the carbon balance of a young ponderosa pine plantation. *Agric. For. Meteorol.* **2005**, *130*, 207–222.
 - 40. Goulden, M.L.; J.W. Munger; S.M. Fan; B.C. Daube; S.C. Wofsy. Measurements of carbon sequestration by long-term eddy covariance: Methods and a critical evaluation of accuracy. *Glob. Chang. Biol.* **1996**, *2*, 169–182.
 - 41. Kwon, H.; B.E. Law; C.K. Thomas; B.G. Johnson. The influence of hydrological variability on inherent water use efficiency in forests of contrasting composition, age, and precipitation regimes in the Pacific Northwest. *Agric. For. Meteorol.* **2017**.
 - 42. Schmid, H.P.; C.S.B. Grimmond; F. Cropley; B. Offerle; H.-B. Su. Measurements of CO₂ and energy fluxes over a mixed hardwood forest in the mid-western United States. *Agric. For. Meteorol.* **2000**, *103*, 357–374.
 - 43. Suyker, A.E.; S.B. Verma; G.G. Burba; T.J. Arkebauer. Gross primary production and ecosystem respiration of irrigated maize and irrigated soybean during a growing season. *Agric. For. Meteorol.* **2005**, *131*, 180–190.
 - 44. Suyker, A.; S. Verma; G. Burba; T. Arkebauer; D. Walters; K. Hubbard. Growing season carbon dioxide exchange in irrigated and rainfed maize. *Agric. For. Meteorol.* **2004**, *124*, 1–13.
 - 45. Monson, R.; A. Turnipseed; J. Sparks; P. Harley; L. Scott-Denton; K. Sparks; T. Huxman. Carbon sequestration in a high-elevation, subalpine forest. *Glob. Chang. Biol.* **2002**, *8*, 459–478.
 - 46. Davis, K.J.; P.S. Bakwin; C. Yi; B.W. Berger; C. Zhao; R.M. Teclaw; J. Isebrands. The annual cycles of CO₂ and H₂O exchange over a northern mixed forest as observed from a very tall tower. *Glob. Chang. Biol.* **2003**, *9*, 1278–1293.
 - 47. Scott, R.L.; J.A. Biederman; E.P. Hamerlynck; G.A. Barron-Gafford. The carbon balance pivot point of southwestern US semiarid ecosystems: Insights from the 21st century drought. *J. Geophys. Res. Biogeosci.* **2015**, *120*, 2612–2624.

48. Scott, R.L.; G.D. Jenerette; D.L. Potts; T.E. Huxman. Effects of seasonal drought on net carbon dioxide exchange from a woody-plant-encroached semiarid grassland. *J. Geophys. Res. Biogeosci.* **2009**, *114*.
49. Desai, A.R.; P.V. Bolstad; B.D. Cook; K.J. Davis; E.V. Carey. Comparing net ecosystem exchange of carbon dioxide between an old-growth and mature forest in the upper Midwest, USA. *Agric. For. Meteorol.* **2005**, *128*, 33–55.
50. Xu, L.; D.D. Baldocchi; J. Tang. How soil moisture, rain pulses, and growth alter the response of ecosystem respiration to temperature. *GBioC.* **2004**, *18*.
51. Hatala, J.A.; M. Detto; O. Sonnentag; S.J. Deverel; J. Verfaillie; D.D. Baldocchi. Greenhouse gas (CO₂, CH₄, H₂O) fluxes from drained and flooded agricultural peatlands in the Sacramento-San Joaquin Delta. *Agric., Ecosyst. Environ.* **2012**, *150*, 1–18.
52. Ma, S.; D.D. Baldocchi; L. Xu; T. Hehn. Inter-annual variability in carbon dioxide exchange of an oak/grass savanna and open grassland in California. *Agric. For. Meteorol.* **2007**, *147*, 157–171.
53. Cook, B.D.; K.J. Davis; W. Wang; A. Desai; B.W. Berger; R.M. Teclaw; J.G. Martin; P.V. Bolstad; P.S. Bakwin; C. Yi. Carbon exchange and venting anomalies in an upland deciduous forest in northern Wisconsin, USA. *Agric. For. Meteorol.* **2004**, *126*, 271–295.
54. Scott, R.L.; T.E. Huxman; W.L. Cable; W.E. Emmerich. Partitioning of evapotranspiration and its relation to carbon dioxide exchange in a Chihuahuan Desert shrubland. *Hydrol. Process.* **2006**, *20*, 3227–3243.
55. Scott, R.L.; E.P. Hamerlynck; G.D. Jenerette; M.S. Moran; G.A. Barron-Gafford. Carbon dioxide exchange in a semidesert grassland through drought-induced vegetation change. *J. Geophys. Res. Biogeosci.* **2010**, *115*.
56. Williams, C.A.; N. Hanan; R.J. Scholes; W. Kutsch. Complexity in water and carbon dioxide fluxes following rain pulses in an African savanna. *Oecologia*. **2009**, *161*, 469–480.



© 2019 by the authors. Submitted for possible open access publication under the terms and conditions of the Creative Commons Attribution (CC BY) license (<http://creativecommons.org/licenses/by/4.0/>).